Journal of Agrometeorology

ISSN : 0972-1665 (print), 2583-2980 (online)
Vol. No. 26 (4) : 395-400 (December - 2024)
https://doi.org/10.54386/jam.v26i4.2663
https://journal.agrimetassociation.org/index.php/jam

Research Paper

Evaluating rice crop phenology and crop yield in hilly region using satellite imagery and Google Earth Engine

SHWETA POKHARIYAL[1,2], N. R. PATEL[2], AJEET SINGH NAIN[1], AKARSH S. G[2]., R. S. RANA[3], R. K. SINGH[1] and RAJEEV RANJAN[1]

[1]*Govind Ballabh Pant University of Agriculture & Technology, Pantnagar, Uttarakhand, India*
[2]*Indian Institute of Remote Sensing, Dehradun, Uttarakhand, India*
[3]*Chaudhary Sarwan Kumar Himachal Pradesh Krishi Vishwavidyalaya, Palampur, Himachal Pradesh, India*
**Corresponding Author: shwetapokhariyal6@gmail.com*

ABSTRACT

Monitoring vegetation phenology is essential for understanding the impacts of climate change on agricultural production. This study leverages Sentinel-2 data to develop an algorithm in Google Earth Engine (GEE) for calculating phenological metrics of rice crop cultivated over the hilly area, allowing for high-resolution, efficient, and large-scale analysis without the need for data download. The study focuses on key metrics, including the start of the season and end of the season, length of growing season derived from various vegetation indices. The results demonstrate that NDVI-based phenological metrics closely align with the observed values at the experimental site, Malan. Moreover, the relationship of NDVI based length of growing season with the rice crop yield was found stronger with a R^2 value of 0.68, depicting the capability of the satellite-based phenology metrics to estimate the rice crop yield in hilly region of Himachal Pradesh.

Keyword: Google Earth Engine, crop phenology, Sentinel-2, crop yield, rice.

Monitoring vegetation phenology is crucial for understanding how vegetation dynamics influence a changing climate (Garonna *et al.,* 2016). As climate change increasingly influences the agricultural production, evaluating the phenology of cultivated lands becomes even more significant. Phenological data are critical for tracking plant development, monitoring agricultural processes, estimating crop yields (Mateo-Sanchis *et al.,* 2021; Prasad *et al.,* 2021), and ensuring food security of the growing global population (Yu *et al.,* 2017), estimating net primary productivity and evaluating the carbon budget of the particular crop (Patel *et al.,* 2023). Additionally, understanding the temporal and spatial variability of phenological changes helps distinguish different vegetation types (Xue *et al.,* 2014; Wang *et al.,* 2013), particularly crops (Wardlow *et al.,* 2008).

Traditionally, plant phenology assessment was carried out through ground-level observations, which involve visual monitoring of the phenological events—a process that is both labor-intensive and time-consuming (Misra *et al.,* 2020). Consequently, space-borne observations have become invaluable for monitoring the spatio-temporal development of plants at a regional scale, typically known as 'land surface phenology' (LSP) (Zeng *et al.,* 2020). LSP is the variation in the seasonal patterns of the vegetated surfaces as observed through remote sensing data (Reed *et al.,* 2009). LSP metrics typically capture the vegetation changes that can be interpreted from the remote sensing imagery. Some of the LSP/ phenology metrics are start of season (SOS), length of growing season, peak of growing season (POS), end of season (EOS) (De Beurs and Henebry 2004), and other transitional stages like maturity and senescence (Zhang *et al.,* 2003). These metrics are usually computed using the normalized difference vegetation index (NDVI) or other common vegetation indices (De Beurs and Henebry 2004; Singh *et al.,* 2022) and are expressed as the day of the year. In India, satellite data has proven capable of delineating phenology metrics for various crops like cotton, sugarcane, and rice (Prasad *et al.,* 2021; Singh *et al.,* 2022), which are primarily cultivated in the plains.

With the advent of "big data" concept, the integration

Article info - DOI: *https://doi.org/10.54386/jam.v26i4.2663*
Received: 17 July 2024; Accepted: 19 August 2024 ; Published online : 01 December 2024

of multi-source and multi-scale remote sensing data, along with the development of robust, efficient, and accurate data processing and comprehensive simulation algorithms, has become a major challenge in remote sensing applications. In this context, Google Earth Engine (GEE) has emerged as a powerful high-computing platform, making it well-suited for addressing the complexities of remote sensing based big data processing (Lonare *et al.,* 2022; Soni *et al.,* 2023; Choudhury and Bhattachrya, 2023). These positions GEE as one of the most promising tools for future applications.

Hilly areas are sensitive indicators of climate change, making it crucial to monitor them for developing effective adaptation and mitigation policies (Orusa *et al.,* 2023). Therefore, it is essential to focus scientific research and climate adaptation strategies on hilly regions to ensure stability in context of the future climate projections (Samuele *et al.,* 2021; Orusa *et al.,* 2023). Among the many impacts of climate change on plants, the most discernible effects are the shortening of the growth period and delay or advancements of major phenological events in the crop growth cycle. As a result, studying crop phenology is becoming increasingly important. To date, as per our knowledge, there have been no phenological studies conducted on crops in hilly regions of India. Consequently, the objective of the study is to estimate phenology metrics from rice crop cultivated in a hilly region using fine-resolution satellite imagery. Terrace farming is commonly practiced in these areas, where the small field sizes necessitate the use of fine-resolution imagery for accurate metric extraction. Additionally, evaluating the performance of multiple vegetation indices for phenological studies typically requires downloading large-area image datasets, which can be time-consuming. In this context, the Google Earth Engine (GEE) platform was employed to obtain the phenology metrics for rice crops using different vegetation indices. Furthermore, this study investigates the relationship between crop yield at various locations in the study area and the corresponding phenology metrics.

MATERIALS AND METHODS

Study area

The area selected for estimating phenology metrics comprises three sub-districts of Kangra district in Himachal Pradesh, where hill agriculture or terrace farming is practiced. This region spans over latitudes 31.88° to 32.39°N and longitudes 76.03° to 76.64°E, covering 2091 square kilometers. The altitude of the study area varies from 350 meters to 1500 meters. The annual rainfall varies from 1500 mm to 1800 mm. The immediate neighboring districts are Mandi to the east, Chamba to the north, Hamirpur and Una to the south, and Pathankot in Punjab to the west. Maize and rice are the major crops produced in this region and forms the backbone of its economy. Other crops grown include wheat, mustard, potatoes, tomatoes, peas, and various others.

Satellite data

Sentinel-2 satellite data has been utilized in this study to calculate the phenological metrics. These metrics were derived using the vegetation indices (VIs) like NDVI, Enhanced Vegetation Index (EVI), Normalized Differential Phenology Index (NDPI). The Sentinel-2 dataset was employed for these calculations. The preparation of satellite data and phenology modeling were conducted in the Google Earth Engine (GEE) platform. The formula used to calculate various indices is as follows:

$$NDVI = \frac{\rho_{nir} - \rho_{red}}{\rho_{nir} + \rho_{red}}$$

$$EVI = 2.5 * \left(\frac{\rho_{nir} - \rho_{red}}{\rho_{nir} + 6 * \rho_{red} - 7.5 * \rho_{blue} + 1}\right)$$

$$NDPI = \frac{\rho_{nir} - (\alpha * \rho_{red} + (1 - \alpha) * \rho_{swir})}{\rho_{nir} + (\alpha * \rho_{red} + (1 - \alpha) * \rho_{swir})}$$

where, ρ_{nir}, ρ_{red}, ρ_{blue}, ρ_{swir} are the NIR (Band 8), RED (Band 4), BLUE (Band 2) and SWIR (Band 11) bands from Sentinel 2. The value of α was set to 0.51, as it was considered as the most effective value for suppressing the variability of the soil backgrounds (Dong *et al.,* 2020).

Field data

An experimental site is located at the Malan Rice and Wheat Research Centre in Palampur, Kangra, Himachal Pradesh (32.1148° N, 76.4162° E), representing a rice-wheat cropping system. The start and end of the growing season were also recorded at the experimental site. In October 2022, a field campaign was conducted in the *Kangra* district to measure crop yield. A total of 21 locations were selected across the study area for this purpose. Plant samples were collected from a 1-meter square area and then sun-dried. The grains were separated from the samples and weighed using a weighing balance. The weights obtained, initially in grams per meter square were subsequently converted to tonnes per hectare (t ha^{-1}) to determine the final crop yield. Additionally, wherever possible, the information about date of transplanting (DOT) and date of harvesting (DOH) were collected from farmers as secondary data. The coordinates of the fields where these dates were recorded during the field campaign are as follows :1) 32.08°N, 76.47°E; 2) 32.12°N, 76.41°E; 3) 32.18°N, 76.31°E; 4) 32.15°N, 76.45°E; 5) 32.16°N, 76.31°E; 6) 32.19°N, 76.19°E; 7) 32.00°N, 76.46°E. The DOT and DOH noted, will hereafter be referred to as observed SOS and observed EOS, respectively.

Methodology

In this study, a vegetation indices-based threshold method was utilized (Bolton *et al.,* 2020; Bornez *et al.,* 2020). This method identifies SOS and EOS as the first and last days, respectively, when a specified threshold value is surpassed. Consequently, LOS is computed as the number of days between SOS and EOS. The value of the threshold, τ, can be kept constant or set dynamically for each pixel (Borgogno-Mondino *et al.,* 2022). For this study, the dynamic threshold value for each pixel was calculated using the approach adopted from Orusa *et al.,* (2023):

$$\tau = \varphi * (minVi - maxVi) + minVi$$

where τ is the dynamic threshold value which depends on the annual amplitude of the time series; $minV_i$ and $maxV_i$ represents the minimum and maximum values of the vegetation index during the crop growing season, respectively. The value φ was adopted as 0.5, representing the mid green-up and mid green-down during the crop growth cycle (Bolton *et al.,* 2020)

To minimize noise, the time-series data was filtered and smoothed before extracting the phenological metrics, following

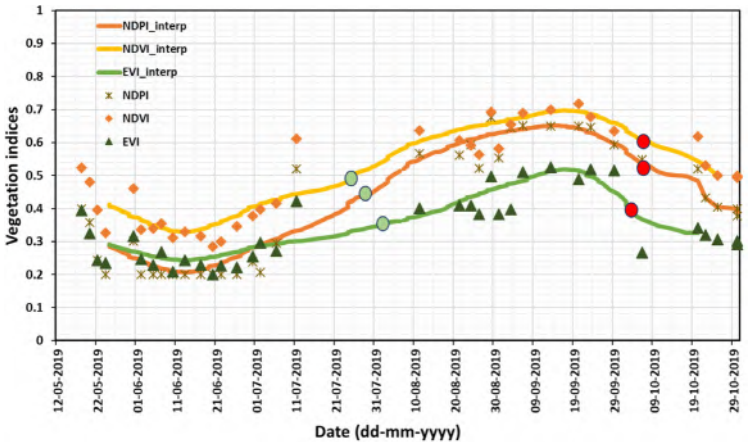

Fig. 1: Temporal profile of NDVI (orange colored diamond), NDPI (brown colored star), and EVI (green colored triangle). The solid line depicts the interpolated time series of the vegetation indices. The green and red circles over the interpolated lines represent the start of the season and the end of the season, respectively, as determined by different vegetation indices.

the approach of Borgogno-Mondino *et al.,* (2022). Time-series of the VIs were first filtered and smoothed for the experimental site. A moving average window of 10 days was applied 20 days to avoid excessive smoothing, which could result in an unrealistic representation of the time series data. If a pixel had no data available within 20-day window, then the window size was extended to 40 days. Following this, cubic spline interpolation was employed to convert the 20-day time series into a daily time series.

Statistical analysis

The accuracy of the estimated metrics from various vegetation indices compared to observed metrics at the experimental site was evaluated by calculating the difference between them. The smallest difference between observed and estimated metrics (from three vegetation indices tested) was identified as most suitable for modeling phenology metrics of rice crop in the study area. The coefficient of variation (CV) in percentage is calculated as:

$$CV\ (\%) = \frac{\text{Mean of the samples}}{\text{Standard Deviation of the samples}}\ x\ 100$$

The relationship between LOS and crop yield was evaluated using linear regression analysis. The coefficient of determination (R^2) was computed to assess the strength of the relationship between these two variables. Additionally, R^2 indicates the proportion of variation in the dependent variable (rice yield) that can be explained by the independent variable (LOS).

RESULTS AND DISCUSSION

Temporal profile of vegetation indices during crop growth cycle

An algorithm was utilized in Google Earth Engine (GEE) to calculate the phenological metrics of the rice crop, enabling dataset processing without the need for downloading, and maintaining a spatial resolution of 10 meters for Sentinel-2. Fig. 1 shows the temporal profile of vegetation indices for the experimental site where phenology was observed in *Kharif* 2022. The figure also depicts the status of the SOS and EOS for the respective vegetation indices in the study area for *Kharif* 2022.

The SOS determined using NDVI occurred earlier compared to the other vegetation indices considered in the study. Specifically, the SOS was modelled on DOY 209 (July 28, 2022), DOY 211 (July 30, 2022) and, DOY 215 (August 03, 2022), when using NDVI, NDPI and EVI, respectively for RS based phenology modelling. At the experimental site, the transplanting data (observed SOS) and harvesting date (observed EOS) for rice during the *Kharif* 2022 was recorded on DOY 192 (July 11, 2022) and DOY 285 (October 12, 2022), respectively. The difference between observed and modelled SOS was 15 days, 17 days and 21 days for NDVI, NDPI and EVI, respectively, indicating that NDVI was more accurate in capturing the SOS of the rice crop at the experimental site. The EOS was modelled using NDVI and NDPI as DOY 280 (October 7, 2022), while EVI indicated the EOS as DOY 276 (October 3, 2022). The difference between the observed and modelled EOS was 5 days for NDVI, NDPI, and 9 days for EVI. This suggests that using EVI resulted in a delayed SOS and an advanced EOS, leading to a shorter growing season for the rice crop. Consequently, the LOS was shortest when using EVI and longest when using NDVI. The difference in observed and modelled SOS is higher in comparison to the observed and modelled EOS, which also reported by Prasad *et al.,* (2021) in cotton crop.

Land surface phenology metrics

The methodology used to extract phenology metrics in GEE effectively captured the crop growth cycle. Fig. 2 illustrates the SOS and EOS for the *Kharif* 2022. While phenological metrics can be computed for any pixel, but they are meaningful on vegetated surfaces where the phenological events takes place. Consequently, this figure displays the phenological metrics for the rice crop only. The SOS and EOS estimated using the NDVI index were found to be in close alignment with the observed values at the experimental site, compared to other indices used in the study. Therefore, Fig. 2 presents the SOS and EOS maps derived from NDVI time series data. The spatial maps indicate that more than 70% of the area for SOS occurs between DOY 194 and DOY 211, and over 80% of the area for EOS falls between DOY 274 and DOY 280. Approximately, 22% of the area shows SOS between DOY 166 and DOY 194, predominantly in the central-eastern portion of the map.

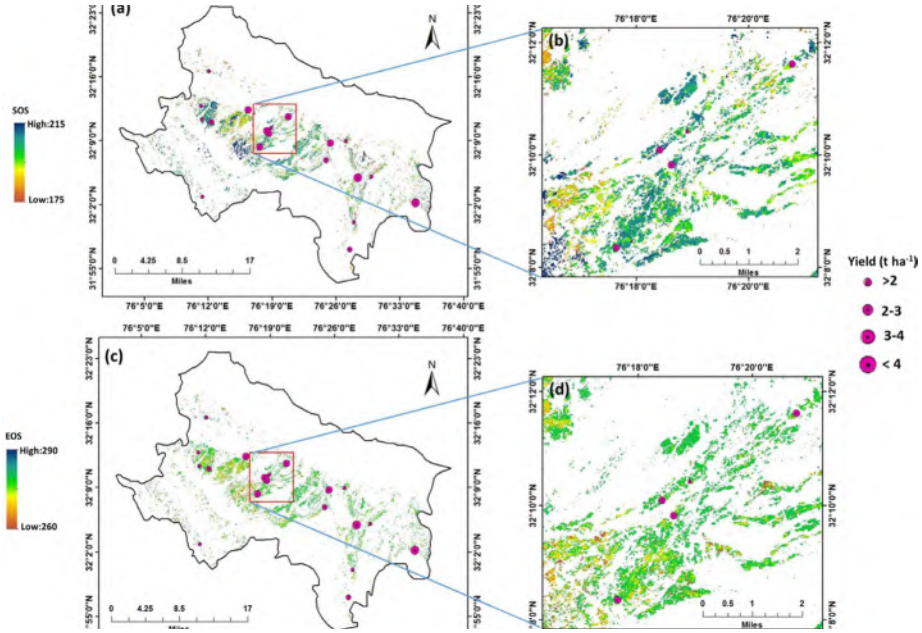

Fig. 2: Start of season (a) and end of season (c) for three sub-districts of the Kangra district in Himachal Pradesh. Panels (b) and (d) provide a zoomed-in view of the area, representing SOS and EOS, respectively. Observed yields at different geographic coordinates are depicted on the maps with pinkcolored circles, where the circle size corresponds to the yield values.

Table 1: Details of the observed and modelled phenology metrics from different locations in *Kangra* region

Site	Latitude	Longitude	Observed SOS	Observed EOS	Modelled SOS	Modelled EOS
1.	32.11°N	76.42°E	192	285	209	280
2.	32.08°N	76.47°E	180	285	175	264
3.	32.12°N	76.41°E	180	282	205	280
4.	32.18°N	76.31°E	176	270	211	280
5.	32.15°N	76.45°E	173	276	198	279
6.	32.16°N	76.31°E	182	280	201	280
7.	32.19°N	76.19°E	176	283	212	280
8.	32.00°N	76.46°E	180	270	209	275
		Mean ± SD	180 ± 5.3	278 ± 5.8	203 ± 11.5	277 ± 5.3
		CV (%)	2.90	2.08	5.60	1.91

During the field campaign, secondary information regarding the observed SOS and observed EOS was collected from the farmers. Table 1 provides details of the observed SOS and observed EOS, expressed as day of the year, from eight different locations. The table also includes the SOS and EOS modelled from the satellite data for the corresponding field locations.

The observed SOS vary across the sites from DOY 173 to DOY 193, while the observed EOS ranges from DOY 270 to DOY 285. The comparison between observed and modelled data reveals how accurately the model captures SOS and EOS. The modelled SOS ranges from DOY 175 to DOY 212, while the modelled EOS varies from DOY 264 to DOY 280. The observed SOS has a CV of 2.90%, whereas the modelled SOS shows a higher CV of 5.60%, indicating more variability in the SOS predictions by the phenology model used in this study. The dataset highlights the discrepancies between the observed and modelled metrics. The mean differences between observed and modelled SOS and EOS suggest that, although the model is generally effective, it may require adjustments to improve its accuracy, particularly for SOS (Prasad *et al.,* 2021; Singh *et al.,* 2022).

While the study provides valuable insights in rice crop phenology, there are some limitations. The present study successfully captures the SOS, EOS, and LOS of the rice growing season, but is not able to account the other stages of rice crop. Further modifications to the GEE code could be made to capture additional stages of rice growth, such as tillering, heading, and maturity. Additionally, the use of Sentinel-2 data in this study has limitations related to time series development, including noise and data gaps (e.g., reduced reflectance due to cloud cover). Finding noise-free values was particularly challenging given the short growing cycle of the rice crop (Soriana-Gonzalez *et al.,* 2022). To address this issue, the combined use of Sentinel-2 and Sentinel-1 data could enhance the prediction of phenological metrics (Mercier *et al.,* 2020). Lastly, this study focuses on a single cropping system and may not be applicable to double cropping systems, which are commonly practiced in India. Future studies can also use daily data on both

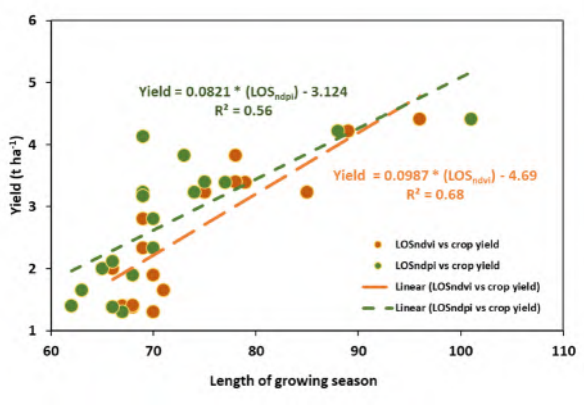

Fig. 3: Relationship between the length of the growing season (LGS) and rice yield. The LGS derived from NDVI (LGSndvi) is depicted using orange circles, while the LGS derived from NDPI (LGSndpi) is depicted using green circles. The relationship between LGSndvi and crop yield is represented by orange colored trend-line, and the relationship between LGSndpi and crop yield is shown with a green colored trend-line.

rainfall and temperature. Additionally, correlating phenology with Growing Degree Days can explain the variability more prominently. The growing degree day is determined by summing the daily temperatures that exceed a set base temperature throughout the year. The base temperature is different for different crops. This approach can capture both temporal and spatial variations in the phenology and delineates the thermal conditions necessary for the crop growth (Wang *et al.,* 2022). Therefore, exploring the spatial variability of phenological metrics in relation to growing degree days could be a promising direction for future research.

Length of growing season and crop yield

The measured crop yield in the *Kangra* district varies from 1.38 t ha^{-1} to 4.41 t ha^{-1}, with the mean of 2.63 t ha^{-1}. The relationship between the LOS and the observed yield was also examined. A comparative assessment was done in between phenology metrics estimated from NDPI and NDVI with extracted values from the geographical coordinates of crop cutting sites. A linear and positive trend was observed between the LOS and rice crop yield (Fig. 3). The relationship was found to be stronger when using NDVI-based phenology metrics compared to NDPI-based phenology metrics, with R^2 values of 0.68 and 0.56, respectively. This suggests that LOS estimated using NDVI time series is more effective in explaining the variability in rice crop yield in the hilly region of Kangra district. The shortening of LOS can lead to shortened vegetative growth period along with decrease in the number of spikelet and grains. It can also impact the decline in the effective accumulated temperature at filling stage, which can lead to lower grain filling thus lowering crop yield (Zhang *et al.,* 2023). Moreover, phenological metrics could also be taken as the dominating influencing factor for crop yield, that can control the carbon allocation between plant organs. Hence, the accurate estimation of the phenological metrics could lead to accurate rice yield estimation at field-scale in the hilly terrain. Guo *et al*., (2020) delineated the dominating influence of phenology metrics on the rice yield. The study also revealed the higher relative importance of phenology than climate on the rice yields.

CONCLUSIONS

This study successfully leveraged Sentinel-2 data to model SOS and EOS of rice crop using the Google Earth Engine (GEE) platform. The algorithm enabled efficient processing of high-resolution spatial data without the need for downloading, facilitating accurate monitoring of the crop growth cycle throughout the season. Our findings highlight that NDVI-based metrics closely matched observed values, proving the utility of remote sensing in capturing key phenological events like SOS and EOS. The relationship between LOS and field-based crop yield was found strong, underscoring the applicability of phenological metrics in estimating crop yield at the field scale. Future research should explore the integration of daily rainfall and temperature data, as well as utilizing growing degree days (GDD), to further enhance the understanding of phenological variability and improve crop monitoring and yield predictions. Additionally, the potential of combining optical and microwave data could be explored for monitoring phenological stages of the crops, particularly during the monsoon season.

ACKNOWLEDGEMENT

We would like to thank Director, IIRS for his kind support. The present study was carried out as a part of Soil & Vegetation Carbon Flux (SVF) project funded by Indian Space Research Organization (ISRO) - Climate & Atmospheric Programme (CAP). Authors sincerely acknowledges CAP office at ISRO Headquarters for facilitating execution of soil & vegetation carbon flux project.

Conflict of Interests: The authors declare that there is no conflict of interest related to this article.

Data availability: Satellite data utilized in this study is accessible through open platforms. Field data can be made available upon reasonable request only.

Authors contribution: **S. Pokhariyal**: Data collection, Data Analysis, Conceptualization, Methodology, Visualization, Writing-original draft, Writing-review; **N.R. Patel**: Resources, Supervision, Writing-review and editing; **A. S. Nain**: Supervision, Writing-review and editing; **Akarsh S.G**.: Data collection; **R.S. Rana**: Data collection, Writing-review; **R.K Singh**: Writing-review and editing; **R. Ranjan**: Writing-review and editing

Disclaimer: The contents, opinions and views expressed in the research article published in the Journal of Agrometeorology are the views of the authors and do not necessarily reflect the views of the organizations they belong to.

Publisher's Note: The periodical remains neutral with regard to jurisdictional claims in published maps and institutional affiliations.

REFERENCES

Bolton, D.K., Gray, J.M., Melaas, E.K., Moon, M., Eklundh, L. and Friedl, M.A. (2020). Continental-scale land surface phenology from harmonized Landsat 8 and Sentinel-2 imagery. *Remote Sens. Environ.,* 240: 111685.

Borgogno-Mondino, E., Farbo, A., Novello, V. and Palma, L.D. (2022). A fast regression-based approach to map water status of pomegranate orchards with sentinel 2 data. *Horti.,* 8(9): 759.

Bornez, K., Descals, A., Verger, A. and Peñuelas, J. (2020). Land surface phenology from VEGETATION and PROBA-V data. Assessment over deciduous forests. *Int. J. Appl. Earth Obs. Geoinf.,* 84: 101974.

Choudhury, I. and Bhattachrya, B. (2023). Assessing the long-term fluctuations in dry-wet spells over Indian region using Markov model in GEE cloud platform. *J. Agrometeorol.,* 25(2): 247-254. https://doi.org/10.54386/jam.v25i2.2184

De Beurs, K.M. and Henebry, G.M. (2004). Land surface phenology, climatic variation, and institutional change: Analyzing agricultural land cover change in Kazakhstan. *Remote Sens. Environ.,* 89(4): 497-509.

Dong, Q., Chen, X., Chen, J., Zhang, C., Liu, L., Cao, X. and Cui, X. (2020). Mapping winter wheat in North China using Sentinel 2A/B data: A method based on phenology-time weighted dynamic time warping. *Remote Sens.,* 12(8): 1274.

Garonna, I., de Jong, R. and Schaepman, M.E. (2016). Variability and evolution of global land surface phenology over the past three decades (1982-2012). *Glob. Change Biol.,* 22(4): 1456-1468.

Guo, Y., Wu, W., Liu, Y., Wu, Z., Geng, X., Zhang, Y. and Fu, Y. (2020). Impacts of climate and phenology on the yields of early mature rice in China. *Sustainability,* 12(23): 10133.

Lonare, A., Maheshwari, B. and Chinnasamy, P. (2022). Village level identification of sugarcane in Sangali, Maharashtra using open-source data. *J. Agrometeorol.,* 24(3): 249-254. https://doi.org/10.54386/jam.v24i3.1688

Mateo-Sanchis, A., Piles, M., Amorós-López, J., Muñoz-Marí, J., Adsuara, J.E., Moreno-Martínez, Á. and Camps-Valls, G. (2021). Learning main drivers of crop progress and failure in Europe with interpretable machine learning. *Int. J. Appl. Earth Obs. Geoinf.,* 104: 102574.

Mercier, A., Betbeder, J., Baudry, J., Le Roux, V., Spicher, F., Lacoux, J. and Hubert-Moy, L. (2020). Evaluation of Sentinel-1 & 2 time series for predicting wheat and rapeseed phenological stages. *ISPRS J. Photogramm. Remote Sens.,* 163: 231-256.

Misra, G., Cawkwell, F. and Wingler, A. (2020). Status of phenological research using Sentinel-2 data: A review. *Remote Sens.,* 12(17): 2760.

Orusa, T., Viani, A., Cammareri, D. and Borgogno Mondino, E. (2023). A google earth engine algorithm to map phenological metrics in mountain areas worldwide with landsat collection and sentinel-2. *Geomatics,* 3(1): 221-238.

Patel, N.R., Pokhariyal, S. and Singh, R.P. (2023). Advancements in remote sensing-based crop yield modelling in India. *J. Agrometeorol.,* 25(3): 343-351. https://doi.org/10.54386/jam.v25i3.2316

Prasad, N.R., Patel, N.R. and Danodia, A. (2021). Cotton yield estimation using phenological metrics derived from long-term MODIS data. *J. Indian Soc. Remote Sens.,* 49: 2597-2610.

Reed, B.C., Schwartz, M.D. and Xiao, X. (2009). Remote sensing phenology: status and the way forward. In: Phenology of ecosystem processes: applications in global change research, 231-246.

Samuele, D.P., Filippo, S., Orusa, T. and Borgogno Mondino, E. (2021). Mapping SAR geometric distortions and their stability along time: A new tool in Google Earth Engine based on Sentinel-1 image time series. *Int. J. Remote Sens.,* 42(23): 9135-9154.

Singh, R., Patel, N.R. and Danodia, A. (2022). Deriving phenological metrics from Landsat-OLI for sugarcane crop type mapping: A case study in North India. *J. Indian Soc. Remote Sens.,* 50(6): 1021-1030.

Soni, A.K., Tripathi, J.N., Ghosh, K., Sateesh, M. and Singh, P. (2023). Evaluating crop water stress through satellite-derived crop water stress index (CWSI) in Marathwada region using Google Earth Engine. *J. Agrometeorol.,* 25(4): 539-546. https://doi.org/10.54386/jam.v25i4.2211

Wang, C., Hunt Jr, E.R., Zhang, L. and Guo, H. (2013). Phenology-assisted classification of C3 and C4 grasses in the US Great Plains and their climate dependency with MODIS time series. *Remote Sens. Environ.,* 138: 90-101.

Wang, X., Liu, Y., Li, X., He, S., Zhong, M. and Shang, F. (2022). Spatiotemporal variation of Osmanthus fragrans phenology in China in response to climate change from 1973 to 1996. *Front. Plant Sci.,* 12: 716071.

Wardlow, B.D. and Egbert, S.L. (2008). Large-area crop mapping using time-series MODIS 250 m NDVI data: An assessment for the US Central Great Plains. *Remote Sens. Environ.,* 112(3): 1096-1116.

Xue, Z., Du, P. and Feng, L. (2014). Phenology-driven land cover classification and trend analysis based on long-term remote sensing image series. *IEEE J. Sel. Top. Appl. Earth Obs. Remote Sens.,* 7(4):1142-1156. https://doi.org/10.1109/JSTARS.2013.2294956

Yu, L., Liu, T., Bu, K., Yan, F., Yang, J., Chang, L. and Zhang, S. (2017). Monitoring the long term vegetation phenology change in Northeast China from 1982 to 2015. *Sci. Rep.,* 7(1): 14770.

Zeng, L., Wardlow, B.D., Xiang, D., Hu, S. and Li, D. (2020). A review of vegetation phenological metrics extraction using time-series, multispectral satellite data. *Remote Sens. Environ.,* 237: 111511.

Zhang, X., Friedl, M.A., Schaaf, C.B., Strahler, A.H., Hodges, J.C., Gao, F. and Huete, A. (2003). Monitoring vegetation phenology using MODIS. *Remote Sens. Environ.,* 84(3): 471-475.

Zhang, R.P., Zhou, N.N., Ashen, R.G., Zhou, L., Feng, T.Y., Zhang, K.Y. and Ma, P. (2023). Effect of Sowing Date on the Growth Characteristics and Yield of Growth-Constrained Direct-Seeding Rice. *Plants,* 12(9): 1899.